Fermi National Accelerator Laboratory

Structure of the Recoiling System in Direct-Photon and π^0 Production by π^- and p Beams at 500 GeV/c

G. Alverson et al
The E706 Collaboration

Fermi National Accelerator Laboratory
P.O. Box 500, Batavia, Illinois 60510

September 1993

Disclaimer

Structure of the Recoiling System in Direct-Photon

and π^0 Production by π^- and

p Beams at 500 GeV/c

G. Alverson,[6] W. F. Baker,[3] G. Ballocchi,[10],[a] R. Benson,[5],[b]
D. Berg,[3] S. Blusk,[9] C. Bromberg,[4] D. Brown,[4] D. Carey,[3] T. Chand,[2]
C. Chandlee,[10] B. C. Choudhary,[2],[c] W. H. Chung,[9] L. de Barbaro,[10]
W. DeSoi,[10] W. Długosz,[6] J. Dunlea,[10] S. Easo,[8],[d] E. Engels, Jr.,[9]
W. Faissler,[6] G. Fanourakis,[10] T. Ferbel,[10] D. Garelick,[6] G. Ginther,[10]
G. Glass,[6] M. Glaubman,[6] P. Gutierrez,[7] K. Hartman,[8],[e] J. Huston,[4]
C. Johnstone,[3] V. Kapoor,[2] I. Kourbanis,[6],[f] A. Lanaro,[10],[g]
C. Lirakis,[6] F. Lobkowicz,[10] P. Lukens,[5],[f] S. Mani,[1] A. Maul,[4] J. Mansour,[10],[h]
R. Miller,[4] C. A. Nelson, Jr.[3] B. Oh,[8] D. Orris,[9]
E. Pothier,[6] E. Prebys,[10],[i] B. M. Rajaram,[2],[j] R. Roser,[10] K. Ruddick,[5]
P. F. Shepard,[9] R. K. Shivpuri,[2] A. Sinanidis,[6] D. Skow,[10],[f] P. Slattery,[10]
L. Sorrell,[4] W. Toothacker,[8] N. Varelas,[10] D. Weerasundara,[9],[k]
J. Whitmore,[8] G. Wu,[6],[f] T. Yasuda,[6] C. Yosef,[6],[h] and M. Zieliński[10]

(Fermilab E-706 Collaboration)

[1] *University of California-Davis, Davis, California 95616*
[2] *University of Delhi, Delhi 11 00 07, India*
[3] *Fermi National Accelerator Laboratory, Batavia, Illinois 60510*
[4] *Michigan State University, East Lansing, Michigan 48824*
[5] *University of Minnesota, Minneapolis, Minnesota 55455*
[6] *Northeastern University, Boston, Massachusetts 02115*
[7] *University of Oklahoma, Norman, Oklahoma 73019*
[8] *Pennsylvania State University, University Park, Pennsylvania 16802*
[9] *University of Pittsburgh, Pittsburgh, Pennsylvania 15260*
[10] *University of Rochester, Rochester, New York 14627*

(a) Current address: CERN, 1211 Geneva 23, Switzerland
(b) Current address: LeCroy Corporation, Chestnut Ridge, NY 10977
(c) Current address: University of California, Riverside, CA 92521
(d) Current address: INFN, University of Perugia, Perugia, Italy
(e) Current address: Stanford University, Stanford, CA 94309
(f) Current address: Fermi National Accelerator Laboratory, Batavia, IL 60510
(g) Current address: INFN, Laboratori Nazionali di Frascati, Frascati, Italy
(h) Current address: Michigan State University, East Lansing, MI 48824
(i) Current address: Princeton University, Princeton, NJ 08544
(j) Current address: L. B. and S. B. S. College, Sagar, Karnatka 577401, India
(k) Current address: Kent State University, Kent, OH 44242

Abstract

We present the results of a study of hadronic jets produced in association with direct photons and π^0's at large transverse momenta in π^-Be and pBe collisions at 500 GeV/c. Using primarily charged particles to characterize the properties of the recoiling jets, we compare their fragmentation and angular distributions, and their correlation with the trigger particle, for both the γ and π^0 event samples. We also compare the data with QCD calculations that incorporate current parton distribution functions.

PACS numbers: 13.85.Qk, 12.38.Qk, 25.40.Ve, 25.80.Ls, 13.85.Ni

Introduction

The production of particles at large transverse momentum (p_T) reflects the dynamics underlying the interactions of the constituents within the colliding hadrons, the momentum distribution of the partons, and their subsequent fragmentation into jets of hadrons. Production of direct photons, in particular, provides an especially clean test of such ideas because, to lowest-order in α_s of perturbative QCD, only the annihilation $(\bar{q}q \rightarrow g\gamma)$ and the Compton $(gq \rightarrow q\gamma)$ subprocesses contribute to the yield of direct photons [1]. The Compton process is very sensitive to the gluon content of hadrons, while the annihilation contribution provides a way of studying gluon fragmentation. The Compton process is expected to dominate direct-photon production in pBe collisions, while both subprocesses are expected to be important in π^-Be interactions. Of course, a greater variety of fundamental subprocesses contribute to π^0 production, and, in fact, high-p_T π^0's result from fragmentations of the scattered partons and not from the primary point-like collisions. Therefore, differences may be expected in the character of the events that involve direct-photon as opposed to π^0 production.

The present data on the structure of the events accompanying high-p_T direct photons or π^0's were obtained as part of the initial run of Fermilab Experiment E-706. A complete discussion of the inclusive production of γ's and π^0's is available in the literature [2]. Here we focus on the correlations between the trigger particle (i.e., the high-p_T γ or π^0) and the accompanying hadrons, as well as on the fragmentation of the away-side jet. We also compare our results with expectations from QCD.

Apparatus and Data Selection

The details of the Meson West spectrometer have been presented elsewhere [3]. Briefly,

2

the detector elements relevant to this analysis include a large-acceptance charged-particle tracking system, consisting of silicon microstrip detectors located upstream, and PWC planes downstream, of a large-aperture dipole magnet, and a highly-segmented liquid-argon and lead electromagnetic calorimeter ($\sim$3 meters in diameter).

To determine the effect of a multi-track environment on the efficiency for reconstructing charged particles, we simulated the detector response using an ISAJET event generator and a GEANT package appropriate to the E-706 geometry [4], and processed the output through our standard reconstruction programs. The quality of agreement between data and Monte Carlo is illustrated in Fig. 1, where we display the distributions in the percentage of the reconstructed tracks as a function of the number of hits observed per charged track in the PWC system. A minimum of 13 out of a possible 16 hits (in 16 planes) was required for any acceptably reconstructed track. Figure 2 displays a comparison of the χ^2 for fits of a trajectory to the hits observed in the PWC planes, as a function of the number of hits per track, for both data and for Monte Carlo. The agreement in Figs. 1 and 2 between the simulations and the measured results gives us confidence in the corrections that we apply for reconstruction inefficiencies in the PWC system.

In characterizing the recoil jets, we have tried different algorithms. We always employ all the charged particles that satisfy the criteria described below, but at times we also include "leading" photons. That is, we use photons to reconstruct away-side jets only when their p_T values exceed those of all the charged particles on the away side. We ignore "non-leading" photons on the away side, because, unlike leading photons, whose reconstruction efficiencies are comparable to those of the trigger photons, softer photons, especially within a jet environment, are less reliably detected. (A discussion of the efficiency for reconstructing γ's and π^0's is given in Alverson et al., in Ref. [3].) Based on simulation studies, the decision to ignore the soft photons does not have great impact on the conclusions of our analysis, nor, for that matter, does the inclusion or exclusion of leading photons.

In reconstructing jets in any event, we define three axes in the center of momentum of the colliding hadrons. One axis is given by the momentum vector of the trigger particle, one is defined by the beam direction, and the third by the momentum vector of the particle of largest p_T emitted in the hemisphere opposite to the trigger. This leading away-side particle can be either a photon (independent of whether that γ originates from a π^0 or η decay, or

3

from any other source) or a charged particle; however, in order to serve as the seed for a recoiling jet, it must have a $p_T > 500$ MeV/c. All the remaining charged particles in the event with $p_T > 300$ MeV/c are assigned to jets along one of the three established axes, depending on their space angle θ_{ik} with respect to those axes. Specifically, for any particle i, and axis k (k=1,2,3), we form the track's axis weight:

$$P_{ik} = \cos\theta_{ik}/(\cos\theta_{i1} + \cos\theta_{i2} + \cos\theta_{i3}) \qquad (1)$$

and we assign each particle to the jet axis k that maximizes P_{ik}. Using these initial assignments, the momentum vectors of the trigger and recoil jets are recalculated by adding the momenta of all the particles assigned to each respective axis. (The direction of the beam jet is not changed, and remains along the beam axis.) Using the new directions for the trigger and recoil jet axes, the P_{ik} weights are calculated again for each particle, and particles are reassigned to their closest jets. After the completion of iterations on this procedure, any particle that does not have a $P_{ik} > 0.35$ (for any of the axes) is dropped from its nearest jet, and ignored in the ensuing analysis. Finally, to be defined as a recoil jet, that jet must be composed of at least two particles, namely a leading and a next-to-leading particle. Based on Monte Carlo simulations of the above analysis procedures, we estimate that the reconstruction efficiency for recoil jets (that is the fraction reconstructed relative to generated) is about 80-85%, and that the uncertainty in the direction of the jet corresponds to $\pm$ 0.15 units in pseudorapidity. Our studies also indicate that, using our jet algorithm, 20-25% of the charged tracks assigned to the recoil jet correspond, in fact, to beam or target fragments. Such improper assignments occur predominantly for recoil jets whose absolute pseudorapidity is large. Unless stated to the contrary, in what follows we restrict our data to center of mass pseudo-rapidities $|\eta| < 0.9$ for both the trigger particles as well as for the reconstructed jets.

Correlations and Fragmentation of Jets

Although jet production dominates hadronic interactions at very large transverse momenta (e.g., at colliders), it is nevertheless quite challenging to extract signals for jets at p_T values below ≈ 10 GeV/c. Figure 3 shows the reconstructed track distribution in the angle ϕ, where ϕ is the difference in the azimuthal angle between the trigger particle and associated charged particle. The results for associated particles with p_T greater than 300 MeV/c are

given for π^0 and for direct-photon candidate events in both π^-Be and pBe data for trigger p_T values above 4.5 GeV/c. The distributions, obtained prior to the reconstruction of jets, are normalized to the total number of events in each sample. The pronounced peak at $\phi = 180°$ suggests the presence of a jet of hadrons recoiling from the trigger particle, and reflects the planar nature of the topology that is characteristic of an underlying two-body hard-scattering process. Because the background from π^0 and η production in the direct-photon samples is substantial at these moderate p_T values, and the γ+jet candidate events have not been corrected for this background, the difference at $\phi = 0°$ between the π^0+jet and γ+jet events is not expected to be large. Nevertheless, the difference is significant, as can be observed in Fig. 3, where the trigger particles in the samples containing direct photons are more isolated in azimuth (i.e., π^0's are accompanied more often than γ's by other particles near $\phi \simeq 0°$). At larger p_T, a greater difference is found to exist between the π^0 and γ triggers, especially in the π^-Be data [6].

The particles within a jet are expected to exhibit short-range correlations in rapidity. To observe such correlations, we examined the rapidity difference ($|\Delta y|$) between the two charged particles with the highest and next-to-highest p_T on the away-side of the trigger particle. (Again, this was done prior to the reconstructing of any jets.) Figure 4(a) displays this difference in rapidity for π^0 triggers with $p_T > 4.5$ GeV/c, and with center of mass $|\eta| < 0.7$. For comparison, the curve shows the same difference in $|\Delta y|$, but "scrambled", namely using particles from different events, and smoothed. The correlations observed in the data are similar to those expected from ISAJET simulations [4]; these are displayed in Fig. 4(b). In the data, as well as in the ISAJET events, the correlations are far stronger between particles within same event (data points) than for different events (smoothed distributions). In Fig. 4(c) we provide a similar comparison based on a multi-particle phase-space Monte Carlo. For this Monte Carlo, we generated events with mean charged-particle multiplicities that matched the data, and with an equal number of π^+, π^-, and π^0 particles, and at least one π^0 with $p_T > 4.5$ GeV/c. (Just as in the data, the p_T of every accepted charged particle had to be above 300 MeV/c, and the particles had to be within our acceptance of $|\eta| < 1.5$.) The results of the multi-particle phase-space Monte Carlo do not indicate the presence of any correlations beyond those expected from constraints in acceptance and kinematics. The observed clustering in rapidity in Fig. 4(a) can therefore be attributed to the production of

jets and to the dynamics of the mechanism responsible for the hadronization process.

The fragmentation of jets can be characterized by the distribution in longitudinal momentum of the remnants of any recoiling jet. We define the fraction of the momentum of a recoiling jet that is carried by any charged particle i as z_i :

$$z_i = \vec{p}_i \cdot \vec{P}_J / P_J^2 \tag{2}$$

where $\vec{P}_J$ is the reconstructed momentum of the recoil jet, and $\vec{p}_i$ is the momentum of the charged particle, both calculated in the overall center of mass frame. The differential multiplicity as a function of z is shown in Fig. 5 for pBe and π^-Be data, separately for γ+jet and π^0+jet events, for values of trigger $p_T > 4.5$ GeV/c. The data for direct photons have been corrected for background from π^0+jet contamination, namely for events where one of the photons from the π^0 either missed or was not reconstructed in the electromagnetic calorimeter. This background was determined using a Monte Carlo program, with our π^0+jet data used as input to calculate the fraction of trigger π^0's that do not reconstruct properly, and are thereby mistaken for direct γ's. This background subtraction procedure is reflected in the data presented in Figs. 5 through 8. Also shown in Fig. 5 are the results of expectations based on an ISAJET simulation of γ+jet and π^0+jet processes [7]. The data are in good agreement with predictions, and there appears to be very little difference between jets accompanying direct photons or π^0's. Moreover, there appears to be no significant difference in fragmentation for direct-photon events using proton and π^- beams. The latter is *a priori* surprising because the nature of the recoiling partons is quite different for the two types of direct-photon events. Nevertheless, similar results have been observed previously [1,8]. In particular, a recent measurement from the OPAL Collaboration at LEP indicates that differences between gluon and quark fragmentations are quite small [9], and beyond the sensitivity of our present level of statistics.

<u>Dynamics of Jets</u>

It has been emphasized by Owens [1] and others that the angular distribution of the recoil jet in the parton-parton scattering frame is particularly sensitive to the dynamics of the production process. Since not all fragments of the recoil jet are identified, we estimate the kinematic variables of the parton collision based upon the reconstructed jet's direction or pseudo-rapidity. We assign the p_T of the trigger particle to that of the recoil jet, which

6

we take to be massless. We then also define a Lorentz boost through a pseudo-rapidity η_B, required for transforming the trigger particle and the recoil jet to their collision rest frame (or, effectively, to the incident parton-parton scattering frame). The variables $\cos\theta^*$, the boost η_B, the p_T, and the energy in the center of momentum of the colliding partons (M) are related to each other, and correlated in their geometrical acceptance. In particular, ignoring rest masses of individual particles and of the partons, the energy in the center of momentum of the colliding partons, or the invariant mass of the (trigger+jet) system, can be written as follows:

$$M = \frac{2p_T}{\sin\theta^*} \tag{3}$$

In Fig. 6 we show the distributions in $\cos\theta^*$, separately, for the π^0 and for the direct-photon data for pBe and π^-Be collisions. (No leading photons were included in reconstructing the recoil jets for the data displayed in Fig. 6.) To minimize the impact of bias in geometric acceptance on the angular distributions, we included events only with $|\eta_B| < 0.3$, and $|\eta_{JET}, \eta_{\gamma,\pi^0}| < 0.85$. Using these criteria, there is no bias in the data for $|\cos\theta^*| < 0.5$, when $p_T > 4.25$ GeV/c and M > 10 GeV/c^2. (The cutoff on M is required to remove the bias in θ^* caused by the single-arm p_T-threshold of our trigger [6].) To enhance the signal to background in the proton data, a p_T cut of 5.0 GeV/c and a corresponding requirement of M > 11.5 GeV/c^2 is employed. All the distributions are normalized to unity at $\cos\theta^* = 0.0$. The results for direct photons show a very weak dependence on $\cos\theta^*$, while the data for π^0 production appear to have a substantially steeper dependence. This difference can be attributed largely to the contribution from the Compton process to direct-photon production, and is similar to previous observation [10]. In fact, our data are in excellent agreement with a simulation based on ISAJET [4] that uses a recent set of leading-log distribution functions for the nucleon [11]. (We should remark that the dependence on θ^* is not very sensitive to small differences in parton distribution functions.) Consequently, we conclude that the shapes of the angular distributions observed for direct-photon and π^0 production can be accommodated in perturbative QCD.

Figure 7 displays the cross sections for trigger+jet production for π^-Be and pBe data, separately for π^0 and for direct-photon yields as a function of p_T. The cross sections are shown averaged over $|\eta_{JET}| < 0.9$ and $|\eta_{\gamma,\pi^0}| < 0.7$. (The recoil jets included those with leading photons on the away side.) The curves on the π^0 data represent leading-log QCD calculations

with an intrinsic k_T of 1 GeV/c [12]. These employ the latest parton distributions of Owens [5,11], with $Q^2=p_T^2/4$ and $Q^2=p_T^2$. The data for direct γs are compared with the next-to-leading log (NLL) calculations [13], using the NLL parton distributions (ABFOW for protons and ABFKW for π^-) that are known to agree with other direct-photon measurements [14]. Here we also used the scales $Q^2=p_T^2/4$ and $Q^2=p_T^2$. The agreement with QCD is poorer at small p_T values, where the calculations are more suspect. We should point out that a previous comparison between NLL calculations [15] and the purely inclusive π^0 and direct-photon cross sections (Alverson et al., Ref [3]) provided a similar level of agreement between data and theory.

The dependence of the cross section on mass might be expected to be more sensitive to correlations between the trigger particle and the recoiling jet than the dependence on p_T alone. In Fig. 8 we display the cross section measured within the acceptance of the apparatus as a function of M for the sets of data shown in Fig. 6. To minimize the impact of different trigger thresholds in our data samples, we plot the results only for $|\cos\theta^*| < 0.4$. This criterion (in addition to requirements on the jet and trigger rapidities of $|\eta| < 0.85$) provides an essentially bias-free cross section as a function of mass. (Leading photons were ignored in the reconstruction of recoil jets used in Fig. 8.) The direct-photon data appear to show a weaker dependence on M than the π^0 data. This can be attributed to the fact that the π^0's originate from the fragmentation of partons. We compare our measurements in Fig. 8 with predictions from ISAJET [4] using the leading-log (LL) parton distribution functions of Duke and Owens DO-I [5] and of Owens [11] for the nucleon, and using Owens [5] for the pion. We have also performed the ISAJET calculations using next-to-leading order ABFOW/ABFKW parton distributions [14]. (It can, of course, be argued that it may be inconsistent to use NLL parton distribution functions in the LL ISAJET calculation, but we did this simply for the sake of completeness.) Below $\approx$ 15 GeV/c^2, the results using ABFOW/ABFKW distributions were found to be essentially the same as those obtained using the latest distributions of Owens [5,11], and are therefore not shown in the figure. Agreement with QCD is observed to be poorer at small mass values, where, again, the calculations are more suspect, and more sensitive to the definition of scale. (Recall that $Q^2 \approx 4p_T^2/3$, and $k_T=1$ GeV/c for ISAJET [4].) The overall agreement in shape between ISAJET and the data is similar for direct-photon and for π^0 production, however, there is

less accord on the normalization for π^0 production. This can be improved somewhat by a change in the definition of scale. We cannot compare our distributions in mass with NLL level calculations because, at present, there is no full Monte Carlo program available for such comparisons, and we therefore look forward to the development of such generators in the future.

References

1. T. Ferbel and W. R. Molzon, Rev. Mod. Phys. **56**, 181 (1984); E. L. Berger, E. Braaten and R. D. Field, Nucl. Phys. B **239**, 52 (1984); J. F. Owens, Rev. Mod. Phys. **59**, 465 (1987).

2. G. Alverson et al, Phys. Rev. Lett. **68**, 2584 (1992) and Phys. Rev. D **45**, 3899 (1992).

3. G. Alverson et al, Phys. Rev. D **48**, 5 (1993); E. Engels, Jr. et al, Nuc. Inst. Meth. **A279**, 272 (1989); F. Lobkowicz et al, Nuc. Inst. Meth. **A235**, 332 (1985).

4. We use ISAJET version V6.36 and GEANT version V3.1305 in these studies. ISAJET defines Q^2 as $2stu/(s^2+t^2+u^2)$, where $s, t,$ and u are the Mandelstam variables for the parton collision. ISAJET also employs an effective k_T smearing, which we have set to 1 GeV/c, to take approximate account of higher-order corrections. Unless specified to the contrary, we use the leading-log parton distribution functions of Duke and Owens Set-1 (DO-I) for the nucleon, and of Owens for the pion [5].

5. D. W. Duke and J. F. Owens (DO-I), Phys. Rev. D **30**, 49 (1984); J. F. Owens, Phys. Rev. D **30**, 943 (1984).

6. D. S. Brown, PhD Dissertation, Michigan State University (1993).

7. We use ISAJET (version V6.36) for this study. Similar results were obtained using PYTHIA version V4.8. See also D. D. S. Weerasundara, PhD Dissertation, University of Pittsburgh (1993).

8. M. Bonesini et al, Z. Phys. C **44**, 71 (1989).

9. P. D. Acton et al, CERN-PPE/93-02 (Z. Phys. C, in press).

10. L. Camilleri, CERN-EP/88-125 (1988); see also F. Abe et al, Phys. Rev. Lett. **71**, 679 (1993).

11. J. F. Owens, Phys. Lett. B **266**, 126 (1991).

12. J. F. Owens, private communication of his Monte Carlo program (1992).

13. H. Baer, J. Ohnemus and J. F. Owens, Phys Rev D **42**, 61 (1990).

14. P. Aurenche et al (ABFOW), Phys. Rev. D **39**, 3275 (1989) and P. Aurenche et al (ABFKW), Phys. Lett. B **233**, 517 (1989).

15. F. Aversa et al, Nucl. Phys. B **327**, 105 (1989); P. Aurenche, et al, Nucl. Phys. B **297**, 661 (1988).

Figure Captions

1. Percentage of the total number of reconstructed tracks as a function of the number of hits per track in the PWC system. The solid line represents the data, and the dashed line a GEANT simulation.

2. Percentage of the total number of reconstructed tracks as a function of the χ^2 per degree of freedom for each fit. The solid lines represents the data, and the dashed lines GEANT simulations for the different number of hits per track.

3. The difference in the azimuth angle between the trigger particle and associated charged particles in the event for proton and π^- data. The associated differential multiplicity are shown separately for direct-photon candidate events (open circles), and for π^0 triggers (filled circles).

10

4. The difference in rapidity between charged tracks that have the highest and next-to-highest p_T on the away side of a π^0 trigger. The data are shown in (a), results of an ISAJET simulation in (b), and results from a phase-space model in (c). The smooth curves correspond to the same differences, but plotted for the highest and next-to-highest charged tracks chosen randomly from different events.

5. The differential multiplicity as a function of the fraction of the momentum of the recoil jet that is carried by charged particles. The distributions are compared to predictions from ISAJET, separately for direct-photon and for π^0 events in proton and π^- data.

6. Angular distribution of the jet in the rest frame of the colliding partons. The distributions are normalized to unity at $\cos\theta^* = 0$. Results from ISAJET calculations for γ and π^0 production in π^- and in proton interactions are shown as dashed curves.

7. The dependence of the cross section on the transverse momentum of the trigger particle for π^0+jet and γ+jet events for proton and for π^- data. The π^0 results are compared with LL calculations [12], and the γ data with NLL calculations [13].

8. The dependence of the cross section on the trigger-jet invariant mass for π^0+jet and γ+jet events for proton and for π^- data. The smooth curves correspond to ISAJET calculations using leading-log parton distribution functions [5,11].
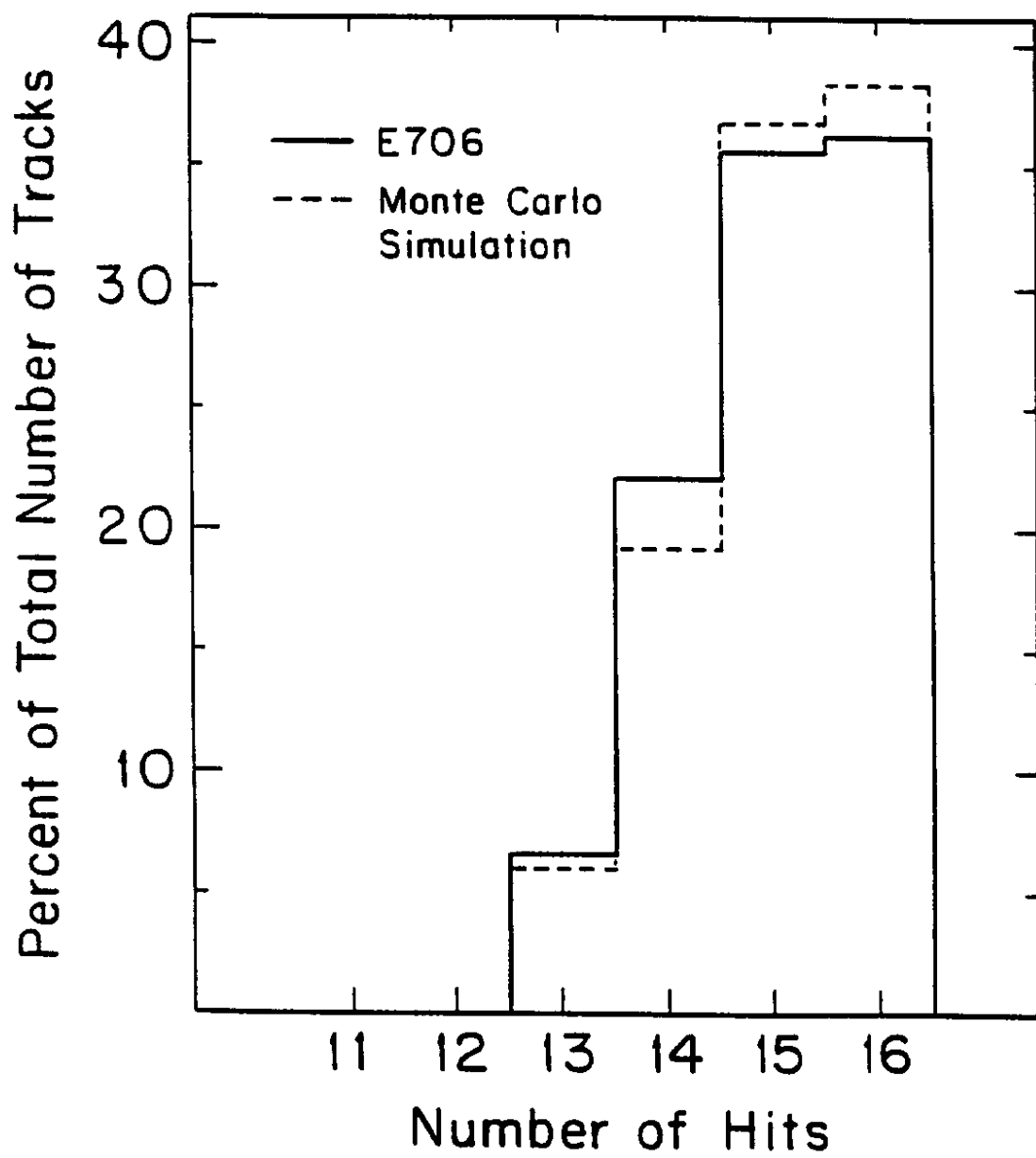
Fig. 1 Percentage of the total number of reconstructed tracks as a function of the number of hits per track in the PWC system. The solid line represents the data, and the dashed line a GEANT simulation.
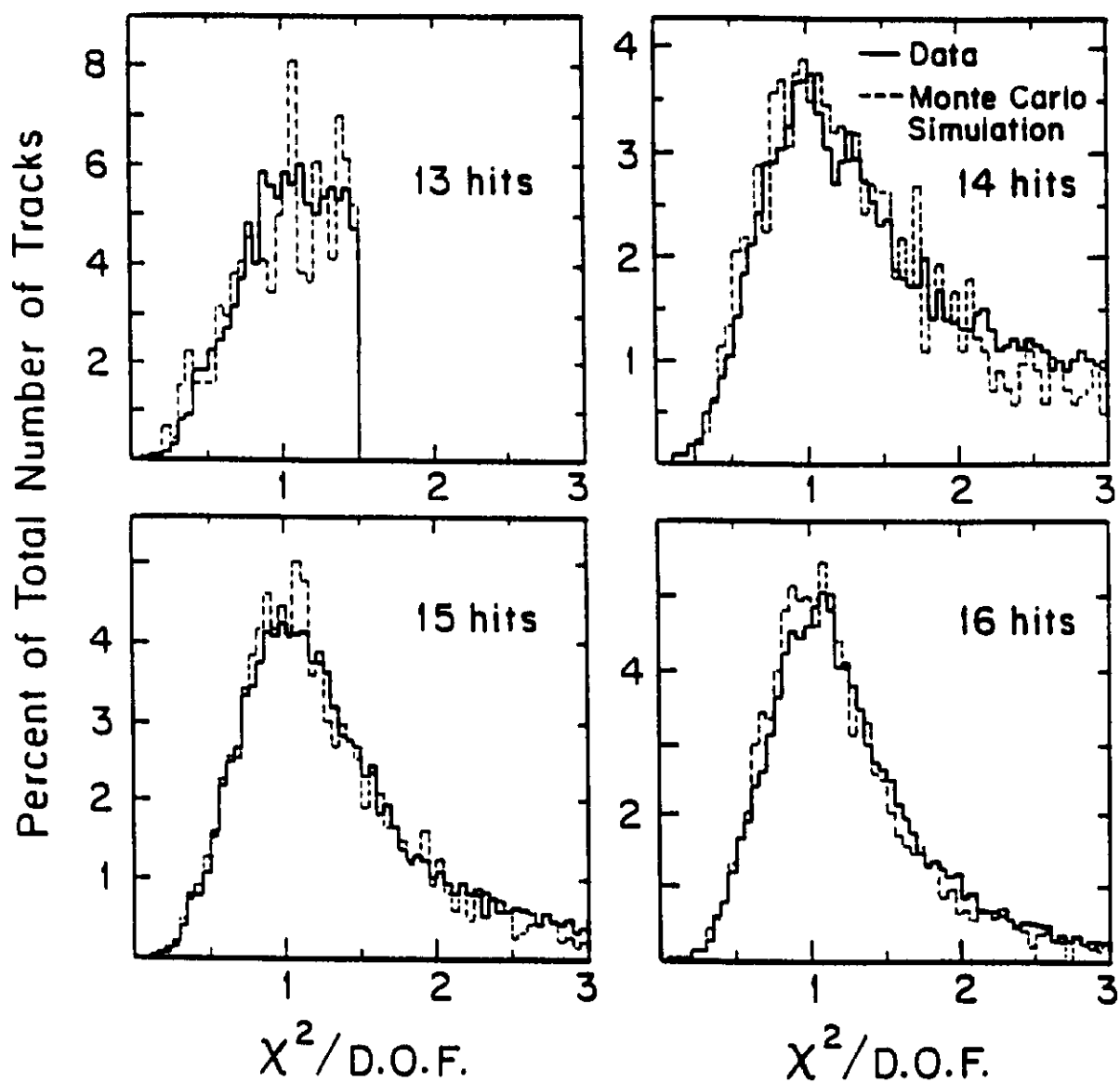
Fig. 2 Percentage of the total number of reconstructed tracks as a function of the χ^2 per degree of freedom for each fit. The solid lines represents the data, and the dashed lines GEANT simulations for the different number of hits per track.
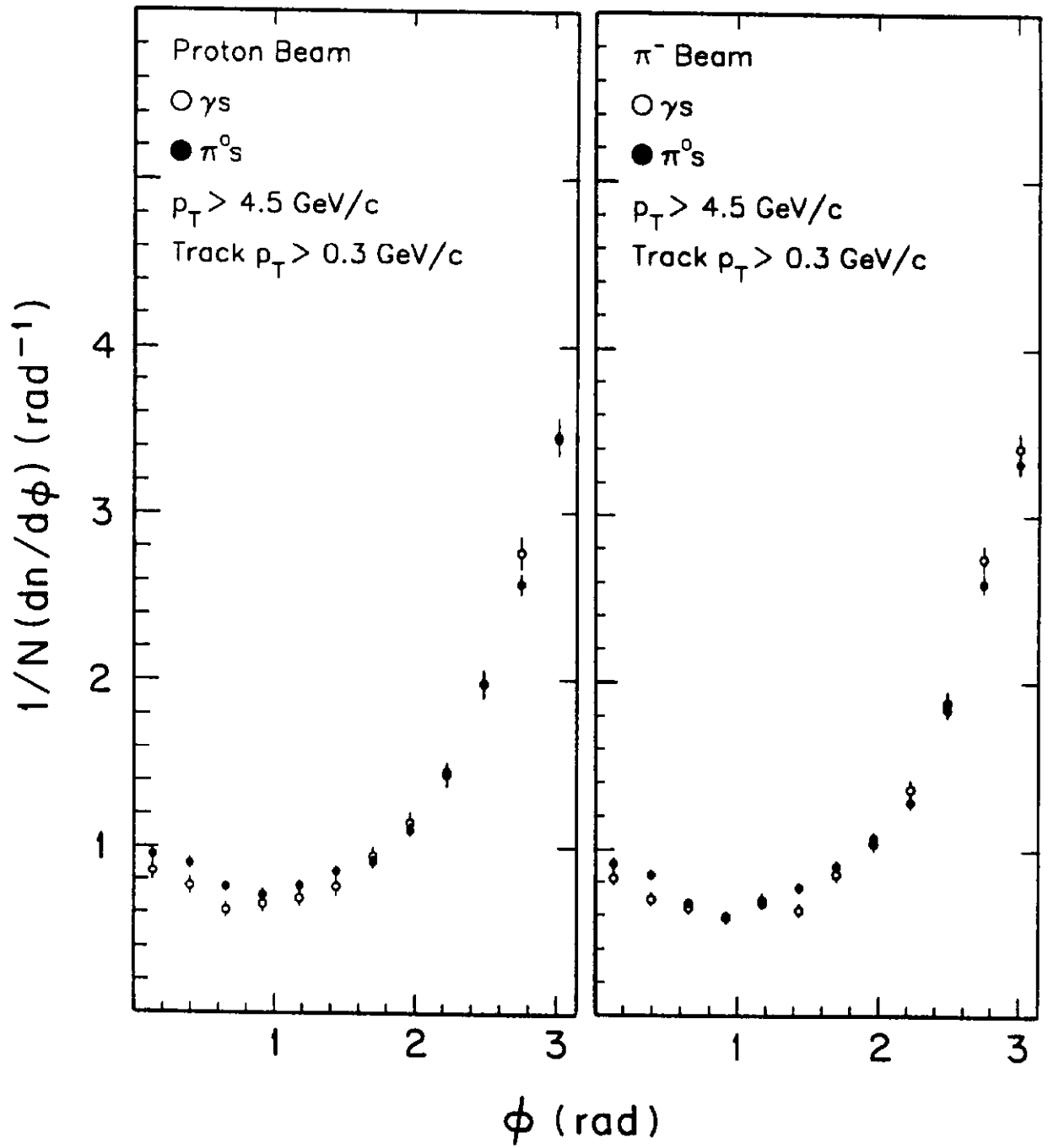
Fig. 3 The difference in the azimuth angle between the trigger particle and associated charged particles in the event for proton and π^- data. The associated differential multiplicity are shown separately for direct-photon candidate events (open circles), and for π^0 triggers (filled circles).
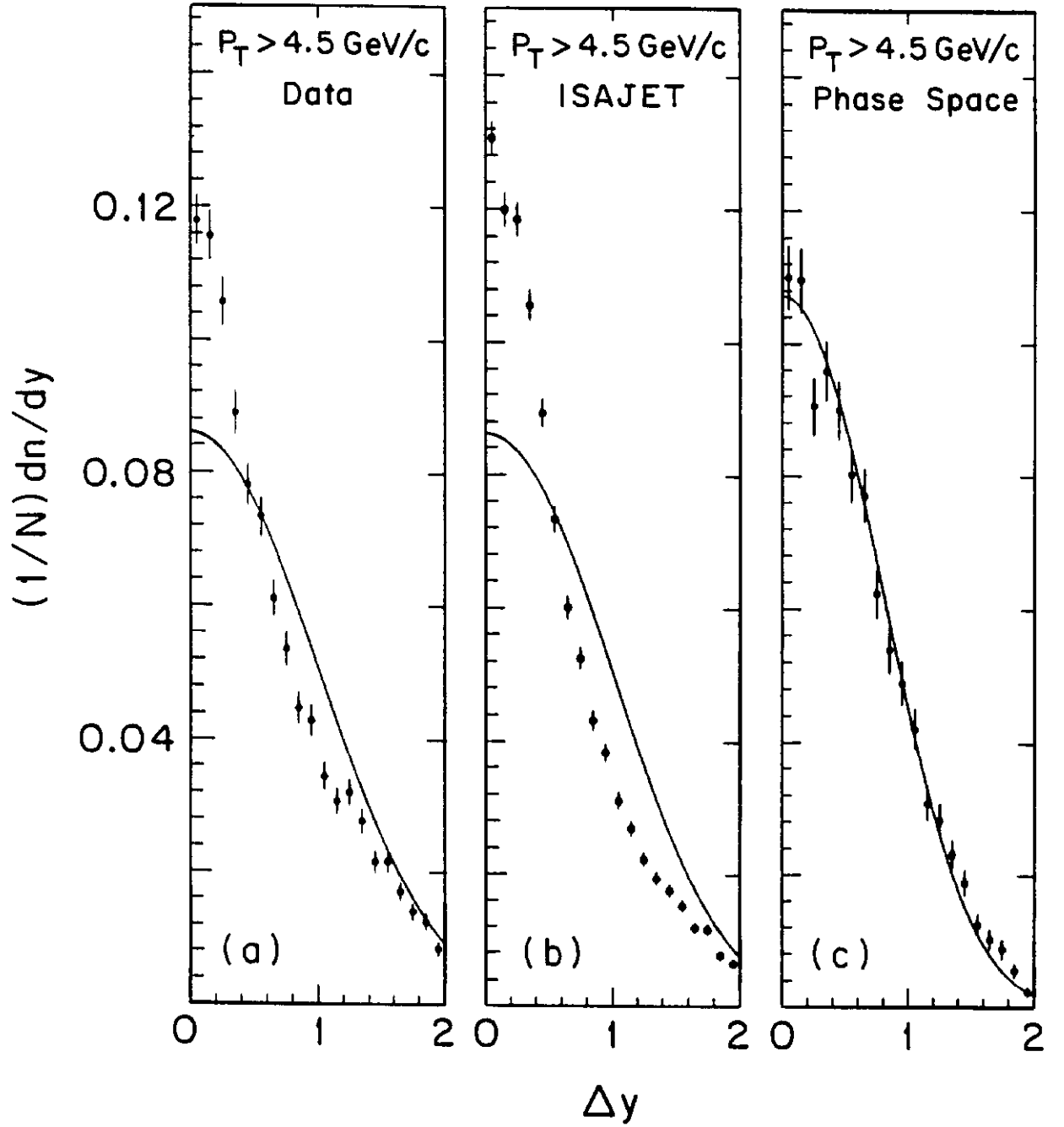
Fig. 4 The difference in rapidity between charged tracks that have the highest and next-to-highest p_T on the away side of a π^0 trigger. The data are shown in (a), results of an ISAJET simulation in (b), and results from a phase-space model in (c). The smooth curves correspond to the same differences, but plotted for the highest and next-to-highest charged tracks chosen randomly from different events.
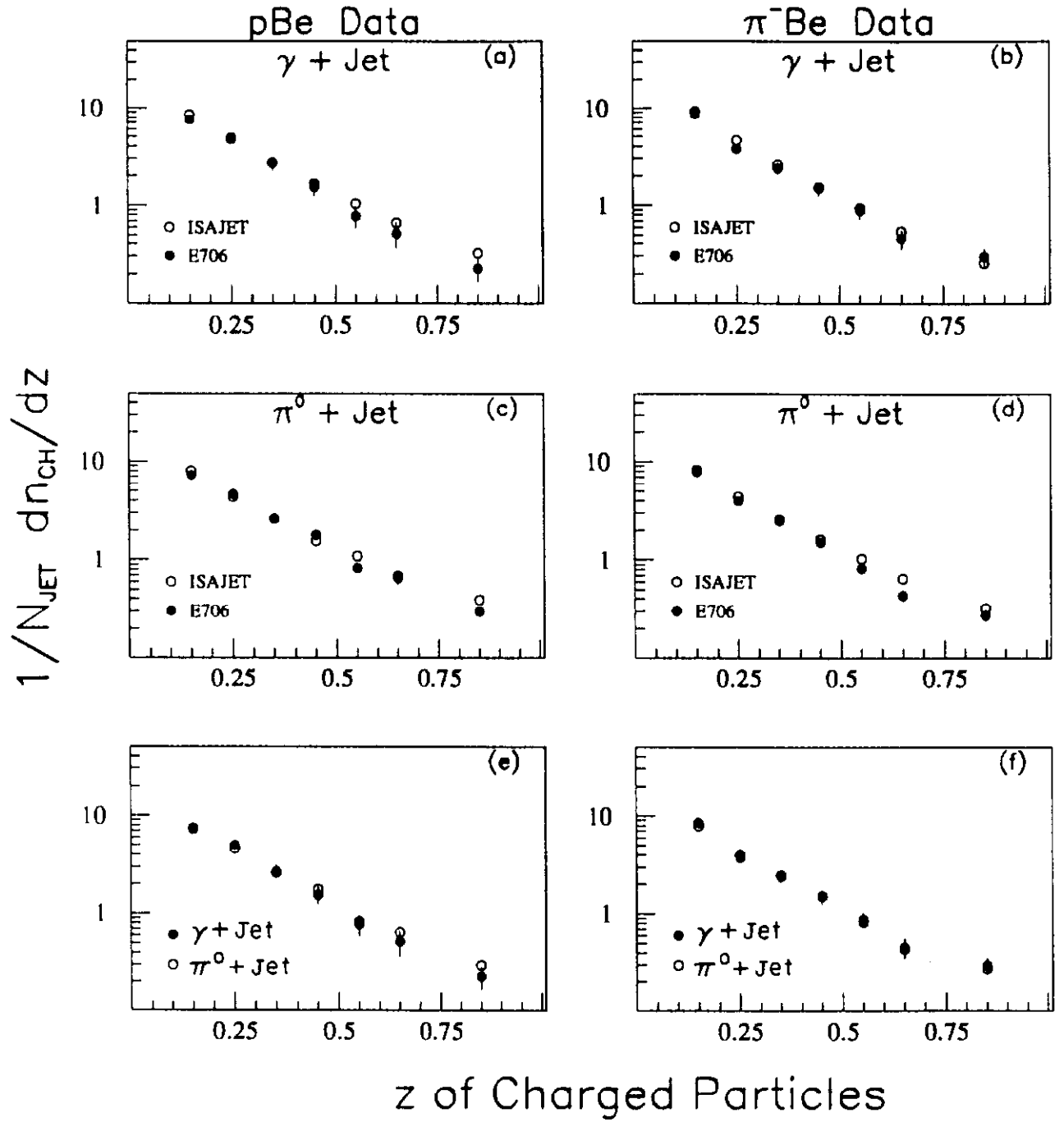
Fig. 5 The differential multiplicity as a function of the fraction of the momentum of the recoil jet that is carried by charged particles. The distributions are compared to predictions from ISAJET, separately for direct-photon and for π^0 events in proton and π^- data.
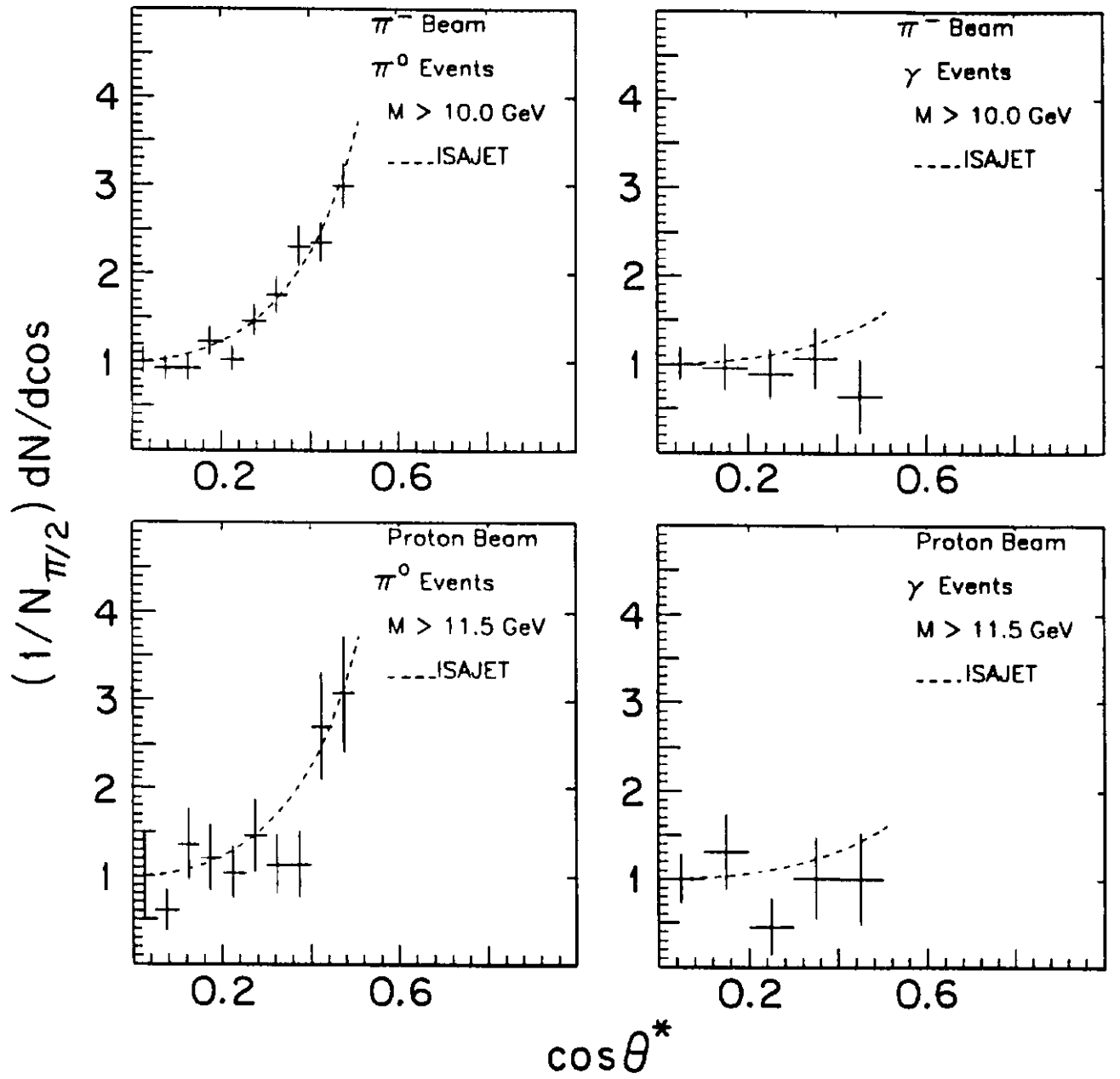
Fig. 6 Angular distribution of the jet in the rest frame of the colliding partons. The distributions are normalized to unity at $\cos\theta^* = 0$. Results from ISAJET calculations for γ and π^0 production in π^- and in proton interactions are shown as dashed curves.
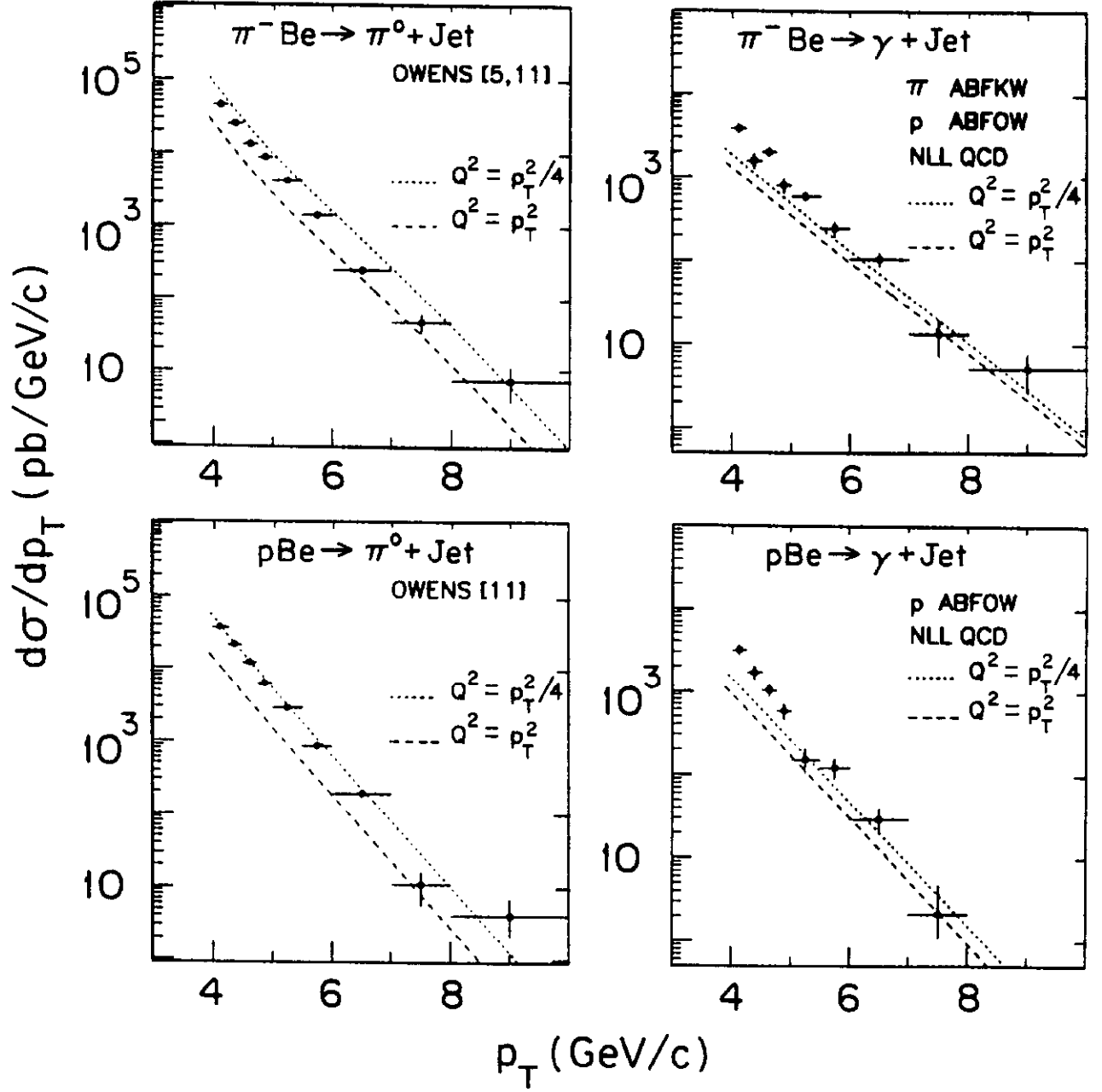
Fig. 7 The dependence of the cross section on the transverse momentum of the trigger particle for π^0+jet and γ+jet events for proton and for π^- data. The π^0 results are compared with LL calculations [12], and the γ data with NLL calculations [13].
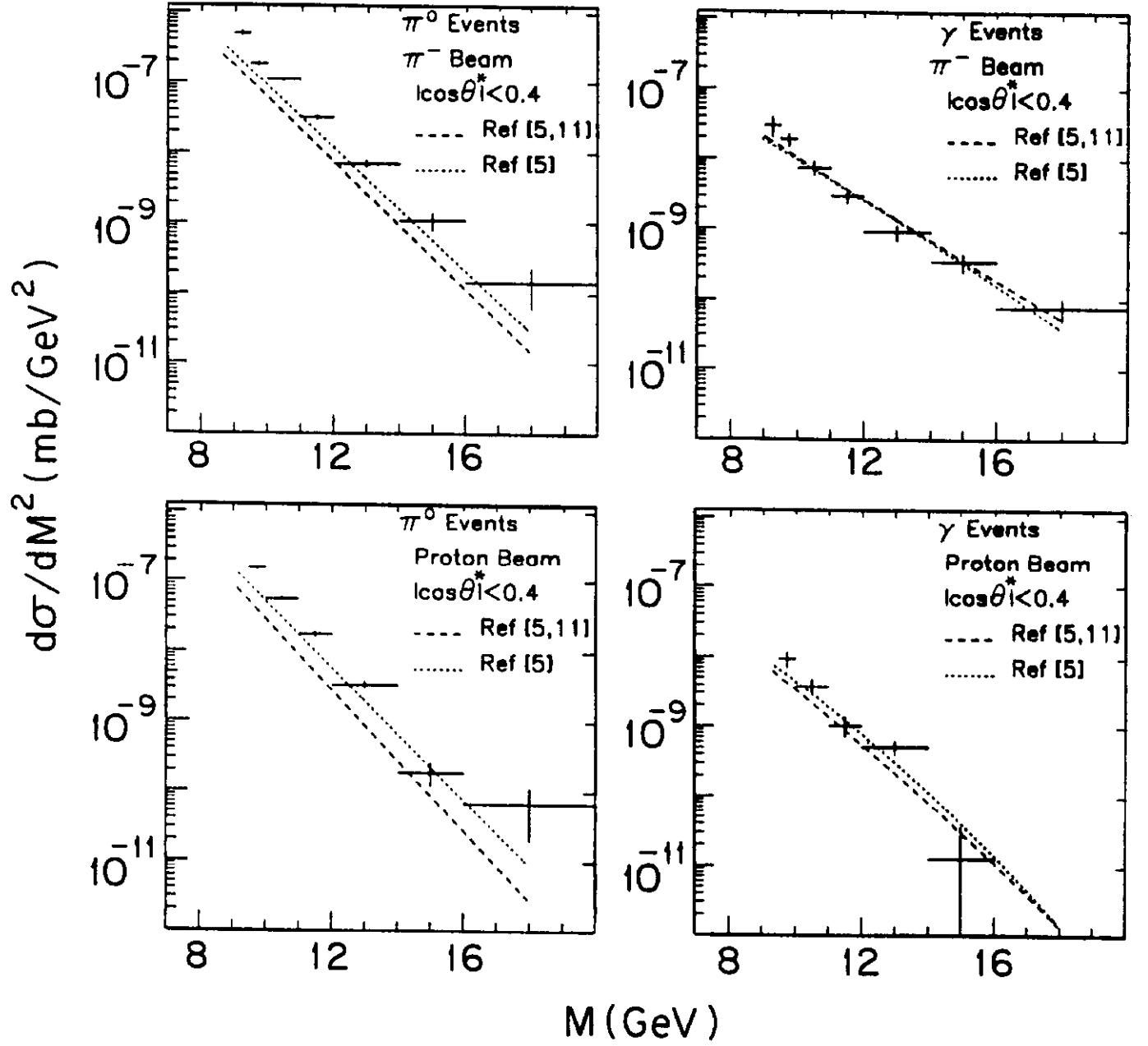
Fig. 8 The dependence of the cross section on the trigger-jet invariant mass for π^0+jet and γ+jet events for proton and for π^- data. The smooth curves correspond to ISAJET calculations using leading-log parton distribution functions [5,11].